New Insights into the Development of Ordered Structure in Poly(ethylene terephthalate). 1. Results from External Reflection Infrared Spectroscopy

Kenneth C. Cole,* Abdellah Ajji, and Éric Pellerin

Industrial Materials Institute, National Research Council Canada, 75 De Mortagne Blvd., Boucherville, Québec, Canada J4B 6Y4

Received August 20, 2001

ABSTRACT: Front-surface external reflection infrared spectroscopy was used to study a set of samples of poly(ethylene terephthalate) (PET) corresponding to various states of order: highly amorphous, drawn at 80 °C to different draw ratios, and thermally crystallized under different conditions. Kramers−Kronig transformation provided high-quality spectra that included an accurate representation of the most intense bands in the spectrum, which are generally saturated or distorted in transmission and internal reflection spectra. Factor analysis indicated the presence of three principal components in the spectra, and by taking linear combinations of the three principal factors, it was possible to generate three distinct physically meaningful basis spectra designated G, TC, and TX. The G spectrum corresponds to a gauche conformation of the ethylene glycol moiety, which is predominant in the amorphous state, while the other two correspond to a trans glycol conformation. The TC spectrum corresponds to the true crystalline state of PET, in which the carbonyl groups are coplanar with and in an all trans arrangement with respect to the benzene rings. The TX spectrum, on the other hand, corresponds to a less ordered trans structure in which the peaks associated with the terephthaloyl moiety of the molecule resemble those observed for the amorphous phase, where the carbonyl groups are either noncoplanar or cis and trans with respect to the benzene rings. However, the TX spectrum is a major contributor in the spectra of the drawn samples. This indicates that drawing at 80 °C produces a structure in which gauche conformers are converted into extended trans sequences, but the terephthaloyl conformation remains rather disordered. In other words, the development of order involves two processes that do not necessarily occur simultaneously. This provides new insight into the nature of the widely reported "intermediate" phase in PET and into the complex behavior of some of the trans peaks in the infrared spectrum. Detailed analysis of the basis spectra, including curve fitting, has also made it possible to suggest more precise assignments for some of the bands in the IR spectrum.

Introduction

Poly(ethylene terephthalate), or PET, is a semicrystalline polymer of considerable commercial importance that is used to make a wide range of products including films, fibers, and bottles. Most of these involve both molecular orientation and crystallization during processing. Despite countless studies of the microstructure of PET and its relationship to process conditions and properties, the complex behavior of this polymer is not fully understood. Because of the relatively slow crystallization rate of PET and the various processing methods used, the products obtained possess a wide range of crystallinity and structures. Highly amorphous PET (less than 5% crystallinity) can be obtained by quenching from the molten state.

Infrared spectroscopy is a valuable tool for studying molecular structure, and there are many examples of its application to PET.[1−15] The molecular conformation plays a very important role in determining the structure of PET. Since the idea was first proposed by Ward,[1−3] it has become widely accepted that the main difference between amorphous and crystalline PET involves the conformation of the ethylene glycol moiety, which through rotation about the C−C bond can exist in either the gauche or the trans form. In fact, it is quite often implicitly assumed that this is the only conformational factor of any significance. However it was pointed out[7,14] that other factors may also be important, like differences in the conformation of the terephthalate moiety resulting from rotation of the carbonyl groups about the carbonyl−phenylene bond. The conformational aspects were considered in detail by Štokr et al.[15] In addition to the gauche (G) and trans (T) forms of the glycol C−C bond, rotation about the C−O bonds of the glycol linkage can likewise lead to gauche (g) and trans (t) conformers. As for the two carbonyl bonds adjacent to each benzene ring, they may lie out of the plane defined by the ring, or they may lie in the plane, in which case they may be in either the cis (C_B) or the trans (T_B) arrangement with respect to each other.

In the crystalline phase of PET, as characterized by Daubeny et al.,[16] the three groups just mentioned are all in the trans conformation (T, t, T_B), and the molecules consist of linear chains in which all the atoms except the hydrogens of the glycol group are practically in the same plane. These "flat" or "ribbonlike" chains pack into a structure with a triclinic unit cell having the dimensions $a = 0.456$ nm, $b = 0.594$ nm, $c = 1.075$ nm, $\alpha = 98.5°$, $\beta = 118°$, and $\gamma = 112°$. The a dimension may be considered to correspond to the ribbon "thickness", b to the "width", and c to the length of a monomer unit. A different structure has been proposed to account for the X-ray diffraction pattern of a mesomorphic form of PET obtained by drawing of amorphous PET below the glass transition temperature.[17−20] It resembles the one just described except that there is rotation about the C−O bonds to give a dihedral angle of about 77°, not far from that of the gauche conformation (g). Molecular modeling indicates that this corresponds to a second state of minimum energy.[19,20]

10.1021/ma011492i CCC: $22.00 Published 2002 by the American Chemical Society
Published on Web 01/03/2002

The amorphous phase of PET is less well characterized, but it is widely accepted that in contrast with the crystalline phase the gauche conformation is predominant for the C−C bond of the glycol group. These gauche units correspond to "kinks" or nonlinearity in the chain. On the basis of data from infrared (IR), Raman, and nuclear magnetic resonance (NMR) spectroscopies, Štokr et al.[15] concluded that the conformational behavior of PET is very similar to that of related model ester compounds. For the amorphous state they estimated the fraction of trans (T) glycol conformers to be 10%; other groups have reported values ranging from 7% to 25%.[21−30] These values were determined by IR or Raman spectroscopy, and the result depends to some extent on which peaks are used and how they are measured (height, area, deconvolution by peak fitting). A recent study by means of two-dimensional NMR gave a figure of 14% trans (T) conformer for the amorphous phase of PET.[31] There appears to be much less information on the conformation around the C−O bond, for which Štokr et al. report 74% trans (t). They also suggest that the carbonyl groups are about equally distributed between C_B and T_B arrangements. Because of resonance stabilization, these coplanar conformations would be expected to be energetically more favorable than nonplanar arrangements, but there has been some discussion on this subject. In their treatment of the configurational statistics of PET chains, Williams and Flory[32] gave equal weighting to the C_B and T_B conformations. However, on the basis of the broad carbonyl band observed at 1730 cm^{-1} in the Raman spectrum, Melveger[33] suggested that amorphous PET contains a range of rotational states in which the carbonyls are rotated out of the plane of the benzene ring by varying amounts. Support for this was provided by Tonelli,[34] whose theoretical calculations showed that although the planar conformations C_B and T_B possess the lowest energy, the barriers to rotation are low and nonplanar conformations are highly probable. Purvis and Bower[35] performed a detailed analysis of the Raman spectrum of oriented PET. They considered two models for the conformation of the terephthaloyl moiety in the amorphous phase: model A, involving only the T_B conformation as in the crystalline phase, and model B, with no preferred orientation of the plane of the ester group with respect to the plane of the benzene ring. It was impossible to unambiguously confirm either model, but model B was slightly favored.

It is thus not surprising that the crystallization of PET is a complex process, as described in a recent review.[36] This is demonstrated by the work of Lin and Koenig,[21,37] who annealed samples of amorphous PET over a wide range of temperatures and times and followed the increase in density as well as the conversion of gauche glycol conformers to trans. When these properties are plotted as a function of log(time) at different temperatures, it is clear that the thermal crystallization of PET involves two distinct stages. The first stage, or primary transformation, starts to proceed at a measurable rate around 90 °C, not far above the glass transition temperature of about 70 °C, and is quite fast at 140 °C. It is characterized by a sigmoidal curve and a constant activation energy of about 170 kJ mol^{-1}. The second stage, or secondary transformation, occurs at a significant rate only above about 160 °C. It is characterized by a linear variation of properties with log(time), it requires much more energy than the primary transformation, and its activation energy varies with temperature according to an Arrhenius-type equation. The differential scanning calorimetry (DSC) thermogram of amorphous PET shows a strong exothermic crystallization peak near 150 °C corresponding to the primary stage of crystallization. For annealed samples that have partly progressed through the primary transformation, this peak moves to lower temperature and decreases in magnitude.[38] At the end of the primary transformation, it disappears and is replaced by an endothermic low melting peak corresponding to the small imperfect crystallites present at this stage. The secondary transformation results in perfection and growth of the crystallites. The difference between the two stages can be seen in the wide-angle X-ray diffraction (WAXD) patterns, where the $(0\bar{1}1)$ and (010) reflections are clearly resolved only in samples that have been treated above 160 °C.[39−41] The two stages of thermal crystallization are also evident in measurements of microhardness, the width of the carbonyl band in the Raman spectrum, and other peaks in the IR and Raman spectra.[23,42,43]

"Strain-induced" crystallization can also be induced in PET, along with molecular orientation, by drawing at temperatures lower than those at which thermal crystallization occurs. The effects of drawing have been widely studied.[25−30,35,44−54] The exact behavior observed depends on the drawing conditions, particularly temperature and strain rate, but it can be described in a general way. When amorphous PET is drawn at temperatures below or near the glass transition temperature, the gauche conformers of the ethylene glycol groups show very low orientation, but the trans conformers orient fairly rapidly in response to the applied stress. Once the few trans conformers initially present are oriented, the stress causes conversion of gauche conformers into new oriented trans conformers. The increase in trans conformers results in more linear chain segments involving extended trans sequences, and when they reach a sufficient length and quantity, they can associate into a more ordered structure. The onset of this "strain-induced crystallization" occurs at a critical value of the draw ratio λ designated as λ_c. The value of λ_c depends on the conditions but is usually around 2 or above.[44−47] It is interesting to note that when PET is drawn around 90 °C at low strain rates, the phenomenon of "flow drawing" is observed.[55] Little stress is required, and there is no conversion of gauche conformers to trans, i.e., no development of crystallinity.[50,51]

It has long been recognized that PET cannot be described very well in terms of a simple two-phase crystalline−amorphous model, and many workers have proposed the presence of a third phase, particularly in drawn products like fibers.[56−59] The nature of this phase has not been clearly defined, and various terms have been used to describe it: intermediate, oriented amorphous, rigid amorphous, constrained amorphous, imperfect crystalline, paracrystalline, mesomorphic with nematic order, etc. (The term "mesomorphic" has also been used to refer to the specific structure mentioned above.) The difficulty in defining this phase arises partly from the fact that its apparent crystallinity depends very much on the technique used to measure it.[59−61] The ordered chains produced by drawing act as precursors for subsequent thermal crystallization, so DSC thermograms of such samples show the same effect observed for samples that have undergone partial thermal crys-

tallization, namely a decrease of the cold crystallization peak and a shift to lower temperature.[46,53] Thus, if DSC is used to characterize the crystallinity, a relatively high value is obtained. On the other hand, the ordered structure is less perfect than the true crystalline structure, so the wide-angle X-ray pattern is rather diffuse; although it is somewhat different from that of amorphous PET, the individual reflections are not resolved as they are for thermally crystallized material.[56,62] A good example of this is shown in a paper by Ellis et al.,[63] where a sample with a draw ratio of 4 gave 31% crystallinity by DSC but a very diffuse WAXD curve. If such a curve is analyzed by the usual methods, a rather low value of crystallinity will be obtained. Density measurements would give yet a different value.[60] Thus, for PET samples drawn at 70 °C, Gupta et al.[49] obtained 26% crystallinity by density measurement but only 7−8% by X-ray. Sharma et al.[61] measured the crystallinity in a set of fibers by various methods, assuming a two-phase model; not only did no two methods give the same result, but not even the same trends were observed. Recently, Bai et al.[64] studied the structural changes induced in PET by mechanical milling and likewise observed that for the milled samples the degree of crystallinity deduced from WAXD was entirely inconsistent with DSC measurements. They postulated an "oriented amorphous" morphology in which the chains are locally aligned but rotationally disordered.

The development of true crystallinity upon thermal treatment of such oriented amorphous PET has been shown to be a complex process. For instance, by combining X-ray diffraction and microhardness measurements, Asano et al.[65] observed the appearance of smectic order at 60 °C, followed by a layer structure around 70 °C, and finally triclinic order above 80 °C. Radhakrishnan and Kaito[66] showed that the isothermal crystallization of oriented PET films at 93 °C involved three stages: thermodynamic relaxation (including gauche−trans conversion), self-organization of the oriented amorphous structure, and crystallization of oriented molecular chains into the crystal lattice. However, an intermediate structure can exist even in the absence of orientation. Imai et al.[67−69] showed that, on annealing of unoriented amorphous PET at 115 °C, a long-range ordered structure with a domain size of 20 nm is formed during the induction period of crystallization. Various NMR studies[70−76] on both oriented and unoriented PET have also indicated the presence of at least three structures, typically designated as mobile noncrystalline (amorphous, gauche rich), constrained noncrystalline (trans rich), and crystalline (all trans). Finally, interesting results obtained recently by in situ X-ray diffraction on a synchrotron beam line during fast drawing of PET have shown the formation of a transient mesophase prior to crystallization.[77−79]

Recently, we[80,81] and other groups[82−85] have shown that front-surface reflection IR spectroscopy can be very useful for studying orientation and structure in polymers. It is particularly interesting because it provides information on the highly absorbing bands that are often saturated or distorted in transmission and attenuated total reflection (ATR) spectra. By means of it, we have observed significant differences between samples with strain-induced crystallinity and one that was thermally crystallized.[86] This prompted us to perform the study reported herein, which includes samples thermally crystallized over a wider range of conditions, to better understand the phenomena that govern the crystallization and structure of PET.

Table 1. Sample Designation and Preparation Conditions

sample	description
Q1	quenched film (amorphous)
Q2	quenched film (amorphous)
Q3	quenched film (amorphous)
Q4	quenched film (amorphous)
D1	drawn at 80 °C to $\lambda = 2.7$
D2	drawn at 80 °C to $\lambda = 3.8$
D3	drawn at 80 °C to $\lambda = 4.5$
H1	heated at 100 °C for 1 h
H2	heated at 120 °C for 10 min
H3	heated at 100 °C for 24 h
H4	heated at 120 °C for 1 h
H5	heated at 200 °C for 15 min
H6	heated at 160 °C for 24 h
H7	slowly cooled from the melt

Experimental Section

The PET used was an extrusion grade without nucleating agent (DuPont Selar PT 7086). An amorphous extruded strip about 3 mm thick was dried at 90 °C for 24 h under vacuum, pressed in a laboratory press at 280 °C, and cooled rapidly in a water bath to give a sheet about 0.5 mm thick with negligible crystallinity (<5%) and orientation. Uniaxially oriented drawn samples (designated D1 to D3) were prepared by drawing the amorphous sheet at 80 °C and 2 cm min^{-1} to different draw ratios (λ) in an Instron tensile tester, followed by rapid quenching in air. Unoriented thermally treated samples (H1 to H7) were prepared by annealing amorphous sheet in an air-circulating oven at different temperatures for different times, except for one sample that was crystallized by slow cooling from the melt. Details on the 14 samples analyzed are given in Table 1.

Infrared spectra with a resolution of 2 cm^{-1} were measured in external reflection at an angle of 11° on a Nicolet Magna 860 instrument with a DTGS detector and a Spectra-Tech model HSR134 reflection accessory. A front-surface gold mirror was used as a reference. For the oriented samples, spectra were measured with the beam polarized both parallel and perpendicular to the draw direction. Kramers−Kronig transformation of the reflection spectra was performed with the use of GRAMS/386 software from Galactic Industries Corp.

Raman spectra were measured on a Nicolet 800 FT-IR instrument equipped with a Raman accessory under the following conditions: Nd:YAG laser (1.06 μm), laser power 0.45 W, 180° backscattering mode, resolution 4 cm^{-1}.

Results and Discussion

Spectra. Front-surface reflection spectra of thick samples generally show derivative-like peak shapes because the reflectance depends (through the Fresnel equations) on both the refractive index n and the absorption index k. Typical reflectance spectra of PET are given in our earlier publications,[80,81] where we took the usual approach of using the Kramers−Kronig relationship to transform the reflectance spectrum into the n and k spectra, the latter of which is similar (but not identical) to the absorbance spectrum obtained by transmission. However, it has been pointed out that, for detailed spectral analysis involving line shapes and intensities, it is better to express the spectrum in terms of the imaginary part of the complex molar polarizability.[87] This quantity, which most reliably gives the molecular properties, is proportional to the following "polarizability function":[26]

$$\phi = \frac{6nk}{(n^2 - k^2 + 2)^2 + 4n^2k^2} \quad (1)$$

For the present work, the GRAMS/386 software was modified to calculate the ϕ spectrum from the n and k spectra. The importance of this is shown in Figure 1, where the ϕ and k spectra are compared for a sample of amorphous PET. For the weaker bands the two spectra are very similar in terms of band shapes and relative intensities, but for the strong bands there are significant differences. In view of this, all the spectra reported here are expressed in terms of the polarizability function ϕ. To correct for variations in overall spectral intensity related to the effects of surface quality, sample positioning, the use of a reference mirror, and so on, the spectra were normalized to a common intensity level by dividing by the area of the band at 1410 cm^{-1}.[80] Previous work involving the ATR technique, where a similar problem exists, indicated that this band is a useful reference band because it is not very sensitive to effects of orientation and conformation.[88]

The assignment of the infrared and Raman peaks of PET has been discussed in various publications.[1−15] Although there were initially some differences of opinion, for most of the infrared peaks there is now general agreement on the assignments proposed by Boerio et al.,[11,12] which in general correspond to those of Miyake.[5,6] Many of the peaks constitute gauche−trans pairs arising from vibrations of the glycol moiety: CH_2 bending at 1453 and 1471 cm^{-1}; CH_2 wagging at 1370 and 1340 cm^{-1}; C−O stretching at 1043 and 972 cm^{-1}; and CH_2 rocking at 899 and 849 cm^{-1}. Others correspond to vibrations of the benzene ring: in-plane vibrations at 1580, 1504, 1410, and 1018 cm^{-1} and out-of-plane vibrations at 875 and 727 cm^{-1}. The complex bands around 1270 and 1100 cm^{-1} are mainly due to vibrations of the ester group. There is also the carbonyl stretching band at 1728 cm^{-1} and a weak peak at 988 cm^{-1} that is specifically related to chain folds in the crystalline phase.[9]

Figure 2 shows the spectra obtained with parallel and perpendicular polarization for the sample D2, drawn at 80 °C to $\lambda = 3.8$. The dichroic behavior is more clearly seen in the difference spectrum shown in Figure 3. Similar results were observed for sample D1 ($\lambda = 2.7$) and sample D3 ($\lambda = 4.5$), except that the magnitude of the dichroism depended on the draw ratio. Although the ϕ spectra shown here differ somewhat from the (lower resolution) k spectra given in our earlier publication,[80] the general behavior is the same. Bands specifically associated with the gauche conformers show low or negligible dichroism, as is generally observed.[26,88−90] Perpendicular dichroism (negative peaks in Figure 3) is observed for the carbonyl band at 1727 cm^{-1} and the out-of-plane ring C−H bands at 873 and 729 cm^{-1}. Parallel dichroism is observed for the trans conformer bands at 1340 and 973 cm^{-1}, the C−H in-plane band at 1018 cm^{-1}, the weak ring bands at 1577 and 1505 cm^{-1}, and the main components of the complex bands around 1265 and 1110 cm^{-1}. For each drawn sample, the spectra $S_{\parallel}$ and $S_{\perp}$ recorded with parallel and perpendicular polarization, respectively, were combined to give the "structural factor" spectrum $S_0 = (S_{\parallel} + 2S_{\perp})/3$. This eliminates the effects of orientation and dichroism and allows one to see the effects of other occurrences like crystallization or conformational changes. Figure 4 compares the structural factor spectra of the drawn samples with that of the original amorphous material. The most obvious effect of the drawing is the decrease of peaks associated with the gauche conformers and the increase of those associated with the trans conformers, especially the CH_2 wagging peak at 1340 cm^{-1}. The

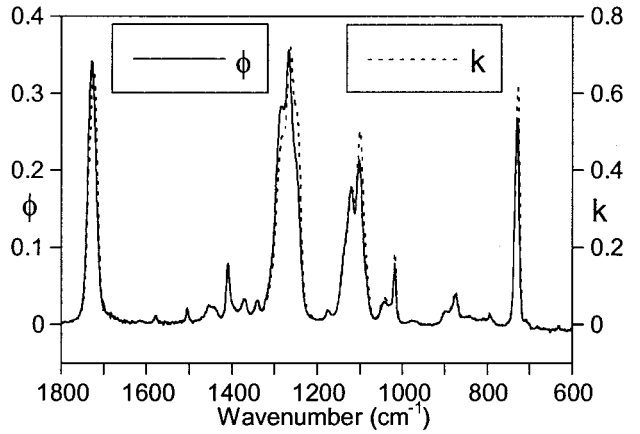

Figure 1. Comparison of ϕ and k spectra for a sample of amorphous PET.

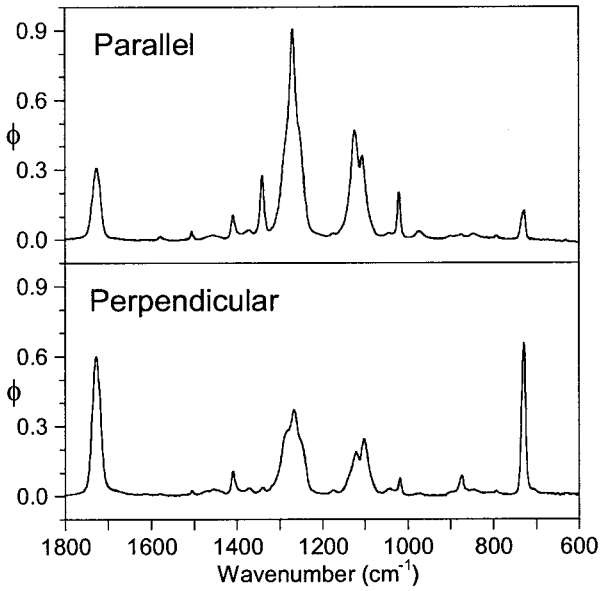

Figure 2. Spectra of drawn PET ($\lambda = 3.8$) measured with polarization parallel and perpendicular to the draw direction.

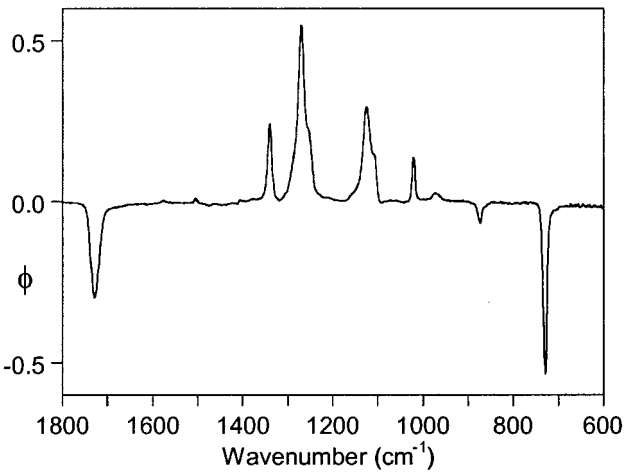

Figure 3. Difference spectrum obtained by subtracting the spectra of Figure 2 (parallel minus perpendicular).

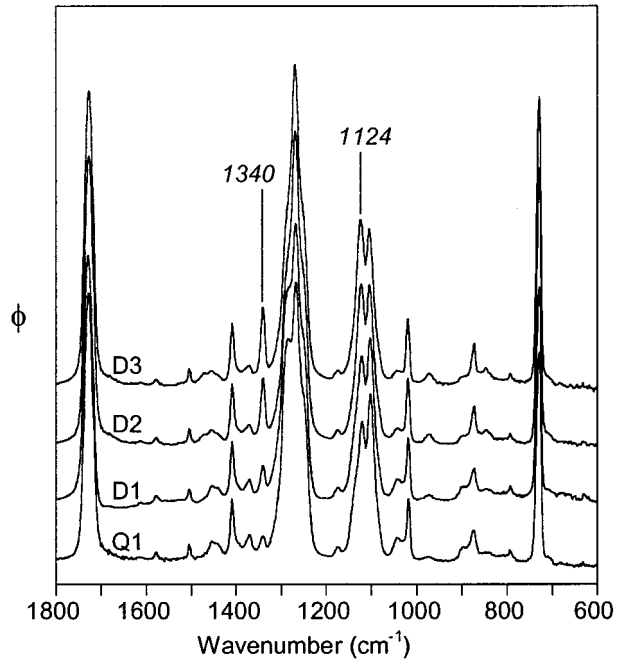

Figure 4. Structural factor spectra of drawn samples D1 to D3 and spectrum of quenched sample Q1.

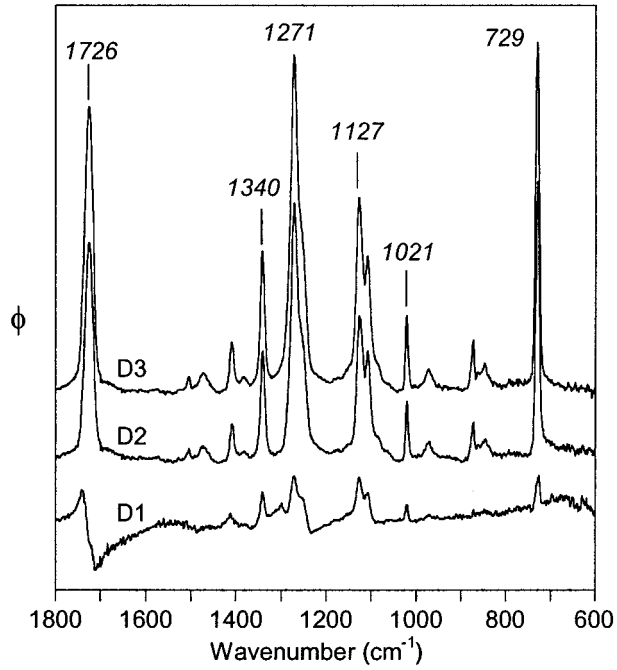

Figure 5. Difference spectra for the drawn samples obtained by subtracting the spectrum of the quenched sample.

complex bands near 1270 and 1100 cm^{-1} change in shape, and the peak at 1124 cm^{-1} increases. By subtracting the spectrum of the amorphous sample from those of the drawn samples and adjusting the subtraction factor until the gauche peaks disappear, it is possible to generate difference spectra corresponding to the trans structure generated by the drawing. These are shown in Figure 5. The difference spectrum for D1 is rather weak and poorly defined, because at this draw ratio the number of trans groups has barely begun to increase. However, it generally resembles the D2 and D3 spectra, which are much better defined and practically identical to each other, except for the difference in intensity.

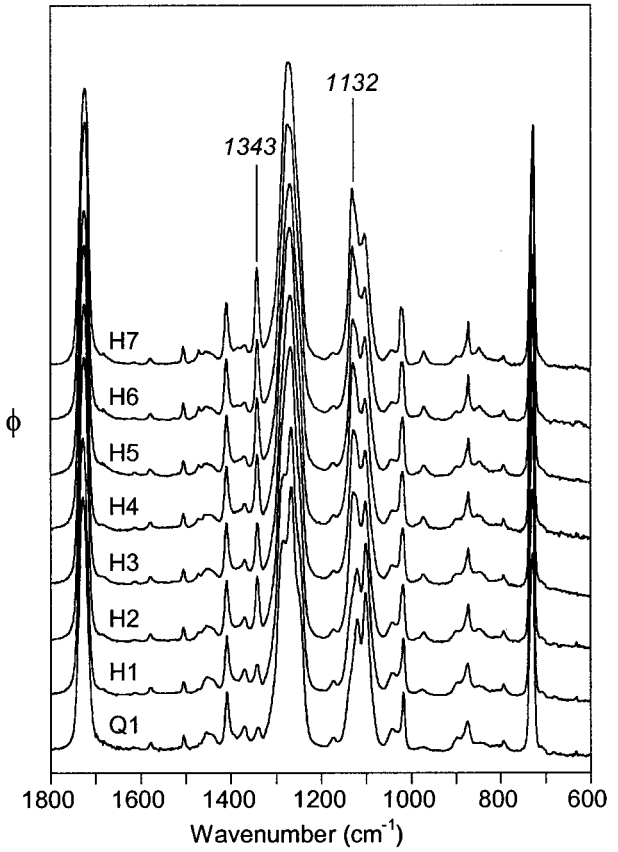

Figure 6. Spectra of heated samples H1 to H7 and quenched sample Q1.

Figure 6 compares the spectra of the various unoriented thermally crystallized samples with that of the amorphous one. The samples and spectra are arranged by order of increasing trans content. Like drawing, thermal crystallization brings about a conversion of gauche conformers to trans. However, comparison with Figure 4 shows certain subtle differences. For example, the trans CH_2 wagging peak now occurs at 1343 cm^{-1}, and the growth of the complex band near 1100 cm^{-1} occurs at 1132 cm^{-1} rather than 1124 cm^{-1}. As was the case for the drawn samples, these changes can be more clearly seen by subtracting out the spectrum of the amorphous sample, as shown in Figure 7. For sample H1, the difference is weak, but for the others it is significant. Close comparison of the difference spectra of Figure 7 with those of Figure 5 leads to an important observation. While both sets of spectra correspond to trans structures and generally resemble each other in overall appearance, there are significant differences in peak shapes and positions. However, within a given set the spectra are quite consistent, regardless of the extent of drawing or thermal crystallization. We can conclude that the trans structure generated by drawing at 80 °C and quenching is significantly different from that generated by thermal crystallization at higher temperatures.

Factor Analysis. To explore this difference in greater detail, factor analysis was performed on the spectra. A similar approach was taken by Koenig and co-workers in their extensive studies on transmission spectra of annealed PET films.[13,21,28,37,38,91,92] The GRAMS/386 software was used to analyze over the range 1800−600 cm^{-1} a set of 14 spectra corresponding to the samples listed in Table 1. (Only the structural factor spectra were used for the three drawn samples.) The

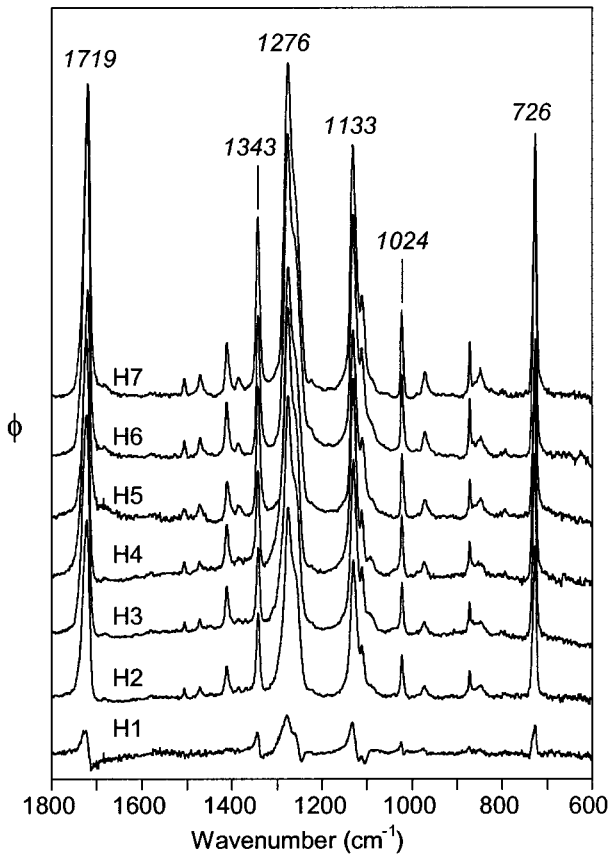

Figure 7. Difference spectra for the heated samples obtained by subtracting the spectrum of the quenched sample.

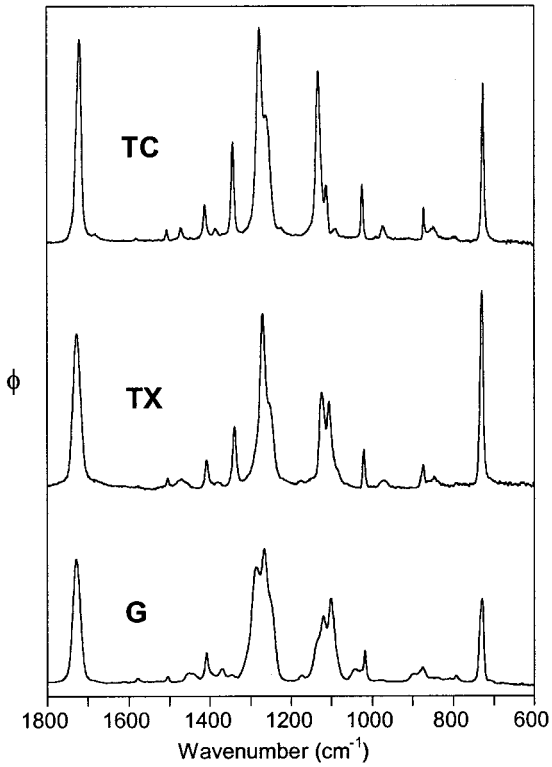

Figure 8. Basis spectra obtained by factorial analysis.

Table 2. Breakdown of Experimental Spectra in Terms of Basis Set

sample	% G	% TX	% TC
Q1	85.2	13.4	1.4
Q2	82.4	13.2	4.4
Q3	82.5	14.6	2.9
Q4	81.5	15.0	3.5
D1	81.8	18.0	0.2
D2	54.2	39.1	6.7
D3	48.2	42.6	9.2
H1	84.3	11.1	4.6
H2	66.6	15.1	18.3
H3	64.7	15.1	20.2
H4	63.4	13.5	23.1
H5	58.0	18.9	23.1
H6	50.2	21.6	28.2
H7	51.5	17.1	31.4

eigenvalues obtained indicated that three principal components, or three distinct factors, account for most of the spectral variation. In other words, all 14 spectra could be well represented by combining these three spectral factors in different proportions. However, these individual factors have no particular chemical or physical significance and often show both positive and negative peaks. In fact, any set of three spectra based on linear combinations of the three primary factors can also serve as a basis set for reproducing the original spectra. By means of spectral subtractions involving the three primary factors, with the help of some chemical intuition and the published literature on PET, we have generated a basis set of three distinct spectra, with well-defined positive peaks, which we believe to have some physical significance. These are shown in Figure 8 and have been normalized with respect to the area of the usual reference peak near 1410 cm^{-1}. The spectrum labeled G (for "gauche") was obtained by eliminating, to the greatest extent possible, peaks known to be associated with the trans conformation of the glycol group, particularly the strong CH_2 wagging peak near 1340 cm^{-1}. However, these peaks could not be eliminated completely without introducing some negative peaks, so some weak features remain at 1347 and 980 cm^{-1}. The G spectrum may be considered therefore to correspond almost exclusively to gauche glycol conformers. The other two spectra, corresponding to trans glycol conformers, were obtained in a similar manner by eliminating peaks associated with the gauche conformers. The spectrum TX possesses a CH_2 wagging peak centered at 1340 cm^{-1} and resembles the difference spectra of the drawn samples in Figure 5, whereas the spectrum TC possesses a peak at 1343 cm^{-1} and resembles the difference spectra of the thermally crystallized samples in Figure 7. Although the same peaks are seen in both of the "trans" spectra, they often do not occur at the same position and are usually narrower in spectrum TC, indicating a more ordered structure. The TC spectrum may thus be considered to arise from the highly ordered trans structure found in the crystalline phase of PET, while the TX spectrum corresponds to a less ordered trans structure.

As previously mentioned, the experimental spectra can be expressed as linear combinations of the three spectra in a given basis set. From the scores calculated in the factor analysis, combined with the coefficients relating our basis set to the primary factors, it was possible to calculate the contributions of our three basis spectra to each of the experimental ones. The results, expressed on a percentage basis, are given in Table 2. If the use of the 1410 cm^{-1} band to normalize our basis spectra is valid, then the figures given in Table 2 can be considered to be an estimate of the percentage of each structure. They confirm quantitatively what is evident from Figures 4−7. The quenched samples contain about

Table 3. Peak Parameters for G, TX, and TC Spectra: Peak Positions in cm^{-1} Followed by Peak Width (Full Width at Half-Height) in Parentheses; Peaks Enclosed in Square Brackets Are Less Well Defined

band	G	TX	TC
C═O stretch	1728.5 (21.5)	1727.3 (21.8)	1719.8 (16.0)
ring def	1577.8 (8.4)		
ring def	1504.9 (7.2)	1504.3 (7.6)	1506.1 (3.9)
CH_2 bending	1454.6 (16.4) Gt?	1470.8 (28.3)	1470.9 (7.6)
	1440.0 (16.9) Gg?		
ring in-plane def	1409.8 (7.7)	1408.7 (8.5)	1412.2 (7.9)
?????	1402.2 (29.1)	[1400.7 (13.3)]	
ring C−H in-plane def		1380.2 (20.6)	1386.0 (13.0)
CH_2 wagging	1370.9 (16.5)	1339.5 (10.4)	1343.0 (7.5)
ring CCH	1314.6 (20.6)		
ring-ester in-plane mode	1287.1 (25.9)	[1274.3 (44.1)]	
glycol O−C−H bending	1265.7 (17.3)	1269.6 (13.1)	1277.5 (15.7)
ring-ester in-plane mode	1248.1 (20.0)	1251.0 (19.7)	1258.5 (18.8)
ring mode or CH_2 twist	1173.8 (17.7)	[1174.5 (26.5)]	
ring mode or CH_2 twist	1135.9 (22.8)	[1149.6 (15.8)]	
ring-ester in-plane mode	1119.8 (15.2)	1123.8 (14.7)	1131.8 (13.2)
in-plane ring mode	1102.1 (15.5)	1106.0 (13.3)	1112.4 (9.0)
glycol C−O stretching (sym)	1091.9 (22.9)	1090.9 (27.2)	
glycol C−O stretching (antisym)	1044.5 (19.0) Gt?	971.2 (20.5)	971.9 (10.9)
	1025.9 (23.5) Gg?		
ring C−H in-plane def	1017.7 (6.2)	1020.1 (6.3)	1023.6 (5.2)
chain folding			989.8 (3.0)
CH_2 rocking	897.0 (21.6)	847.5 (33.0)	850.6 (22.4)
ring C−H out-of-plane def	875.7 (16.1)	873.4 (6.3)	871.9 (3.8)
		878.8 (5.7)	
ring C−H in-plane def?	792.9 (10.2)		
ring C−H + C═O out-of-plane def	729.5 (12.5)	729.5 (9.3)	726.1 (7.2)

83% G, 14% TX, and 3% TC. The main effect of drawing at 80 °C to draw ratios above 2 is to convert G into TX, although a slight increase in TC is also observed. Thermal crystallization, on the other hand, brings about a net conversion of G to TC, with little change in the amount of TX.

D'Esposito and Koenig,[13] by subtraction of spectra of PET films annealed under different conditions, generated difference spectra that they assigned to the crystalline and amorphous components of PET. Their "crystalline" spectrum (the bottom curves in Figures 2 and 4 of ref 13) is identical to our TC spectrum. (It is interesting to note that although front-surface reflection spectra have a higher noise level than transmission spectra, it is nevertheless possible to detect in our TC spectrum some of the finer details described by D'Esposito and Koenig, like the chain folding band at 988 cm^{-1} and the weak peaks at 1685 and 1227 cm^{-1}.) In generating their "amorphous" spectrum, however, D'Esposito and Koenig were unable to eliminate completely the peaks associated with the trans conformer. In fact, examination of their "amorphous" spectrum (the top curves in Figures 2 and 4 of ref 13) suggests that it is in effect a combination of our G and TX spectra. Shen et al.[93] also analyzed a set of PET films annealed at different temperatures and by spectral subtraction produced two distinct trans spectra that they assigned to "crystalline trans" and "amorphous trans". Again, their "crystalline trans" spectrum (Figure 3a of ref 93) is identical to our TC spectrum, while their "amorphous trans" spectrum (Figure 3b of ref 93) resembles our TX spectrum with some G spectrum mixed in. The factor analysis done later by Lin and Koenig[21] indicated the presence of only two principal components in their spectra. By subtracting or ratioing spectra, they were able to generate two clearly distinct spectra corresponding to gauche and trans conformers. There was also some evidence for two types of trans structures, which they associated with the amorphous and crystalline phases. Further support for this came from still later work in which the factor analysis was limited to narrower spectral regions.[92] This made it possible to produce partial spectra corresponding to gauche, amorphous trans, and crystalline trans structures. These spectra possess some of the features seen in our G, TX, and TC spectra, respectively, but again the separation is not as "clean" as in this work. The probable reason for the cleaner separation of the two trans spectra shown here, in comparison with previous work, is that the present study includes drawn samples containing a much higher percentage of TX than thermally crystallized samples, so the TX and TC spectra can be distinguished more clearly.

Discussion of Spectra. The above results show that, where comparison is possible, there is excellent agreement between transmission spectra and front-surface reflection spectra of PET. In a way, front-surface reflection spectra are complementary to transmission spectra, because although the weaker peaks are subject to more noise, the stronger ones are generally better defined and not affected by saturation. The present spectra therefore constitute new data, and it is useful to examine them in greater detail in the light of previous work in order to search for new information on PET. To aid in the interpretation, in some cases attempts have been made to fit the spectra with a minimum number of Pearson VII peaks.[94] Details concerning the peaks in the G, TX, and TC spectra are summarized in Table 3.

The most interesting question to be answered concerns the difference between the TX and TC structures. Some indication comes from the carbonyl stretching band, which is particularly interesting because there is so little prior information available concerning its behavior. Figure 9 shows the carbonyl band in the three basis spectra. In the G spectrum, which is associated with the amorphous phase, it consists of a broad symmetric peak with a perfectly Gaussian shape, centered at 1728.5 cm^{-1} and having a width w (full width at half-height) equal to 21.5 cm^{-1}. In the TX spectrum, it has a similar shape and width but is shifted to slightly

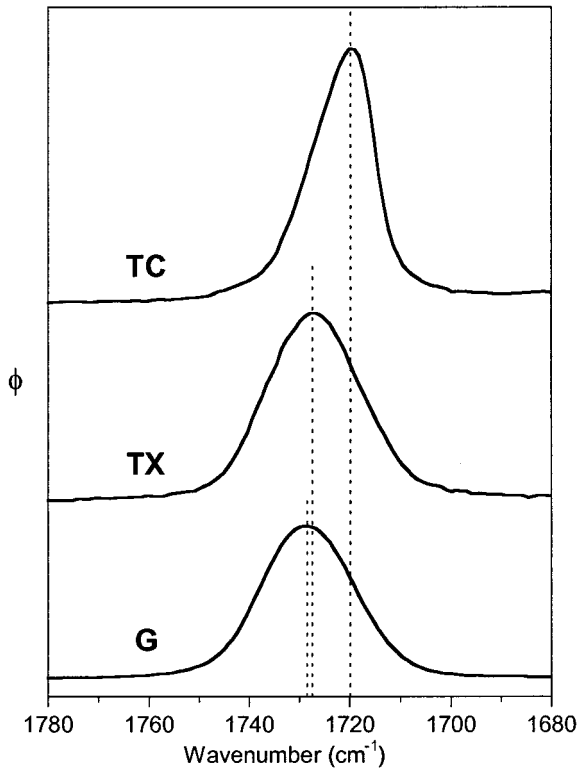

Figure 9. Carbonyl band in the basis spectra of Figure 8.

lower wavenumber (1727.3 cm^{-1}). In the TC spectrum, however, it is decidedly asymmetric, the maximum has shifted considerably to 1719.8 cm^{-1}, and the width is only 16 cm^{-1}. We interpret this to mean that the passage from the G structure to the TX structure, which is the main effect of drawing at 80 °C, involves primarily conversion of gauche glycol conformers to trans, with little change in the conformation of the carbonyl groups. These remain in a rather disordered state with respect to the planes of the benzene rings, as in the amorphous phase. In the TC structure, on the other hand, the carbonyls have undergone more significant changes, leading to more efficient chain packing and a higher state of order as reflected in the narrowing of the carbonyl band. Raman data support this interpretation. Figure 10 shows the carbonyl stretching band in the Raman spectrum of some PET samples similar to those characterized by IR. In the amorphous sample, the band is broad and slightly asymmetric, with a maximum at 1724.6 cm^{-1} and a width of 26 cm^{-1}. On thermal crystallization, the band changes shape and becomes narrower, as observed by Melveger.[33] However, on drawing at 80 °C and quenching, the carbonyl band shows practically no change in shape, as observed in the IR spectra. Similar Raman results for drawn samples were reported by Purvis and Bower.[35] Interesting behavior is also observed in the IR spectra for the strong band near 730 cm^{-1}, shown in Figure 11. In the G spectrum it has a maximum at 729.5 cm^{-1}, a width of 12.5 cm^{-1}, and an asymmetric shape with a high-wavenumber shoulder. In the TX spectrum it loses the shoulder and thus becomes somewhat narrower (w = 9.3 cm^{-1}), but the maximum remains at 729.5 cm^{-1}. In the TC spectrum, however, it shifts to 726.1 cm^{-1} and becomes narrower still (w = 7.2 cm^{-1}). These changes resemble those observed for the carbonyl stretching band. This is not surprising because it was proposed by Miyake[5] and confirmed by the normal-coordinate

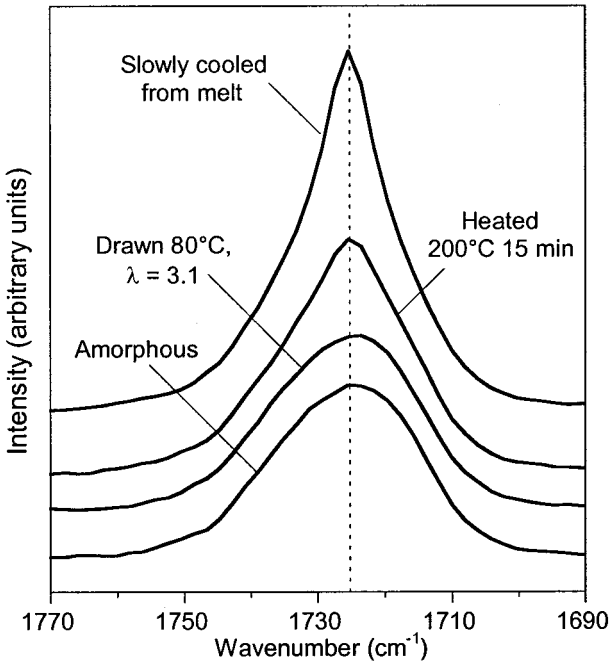

Figure 10. Carbonyl band in the Raman spectra of some PET samples.

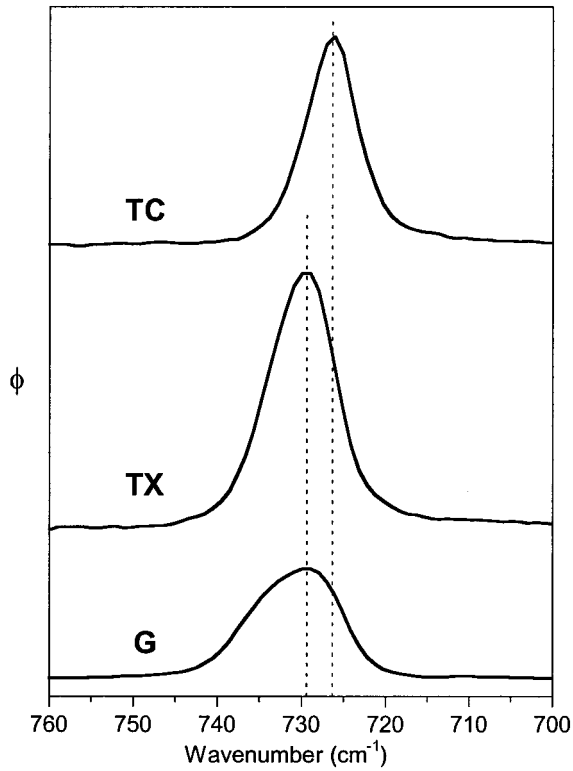

Figure 11. Out-of-plane phenyl C−H peak in the basis spectra of Figure 8.

analysis of Boerio et al.[12] that this band arises from a C═O out-of-plane bending mode coupled with a ring CH out-of-plane bending mode. The CH out-of-plane mode at 875 cm^{-1}, on the other hand, does not involve any contribution from the carbonyl group.[12]

Figures 12−14 show the weaker peaks in the spectrum, which have already been widely studied. Some of these correspond to the gauche−trans pairs mentioned earlier, like the well-known CH_2 wagging mode near 1370 and 1340 cm^{-1} (Figure 12). In the G spectrum

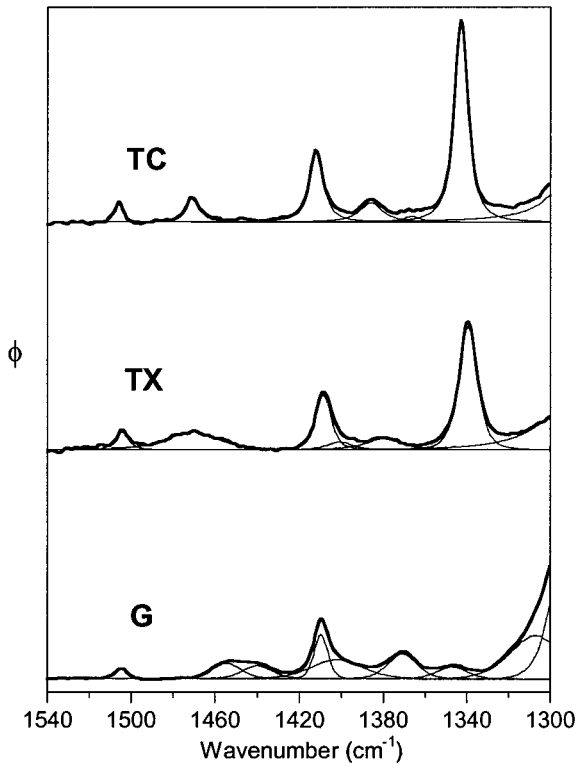

Figure 12. The 1540−1300 cm^{-1} region of the basis spectra of Figure 8.

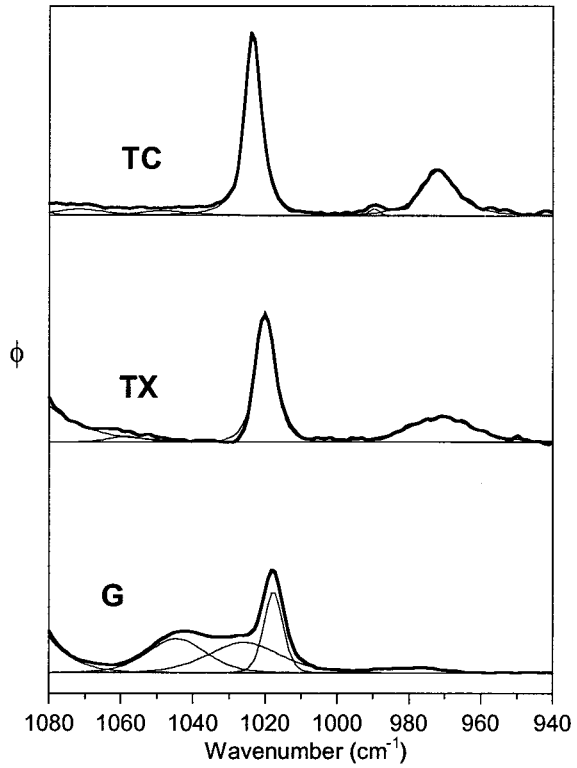

Figure 13. The 1080−940 cm^{-1} region of the basis spectra of Figure 8.

the gauche peak occurs at 1371 cm^{-1}; there is also an apparent residual trans peak at 1347 cm^{-1} that may be significant or may be the result of imperfect separation of the spectra. The most interesting feature here is the trans wagging band in the TX and TC spectra. In both cases it can be represented by a single symmetric peak, but in the TX spectrum it occurs at 1339.5 cm^{-1} and has a width of 10.4 cm^{-1}, whereas in the TC spectrum it occurs at 1343.0 cm^{-1} and has a width of 7.5 cm^{-1}. The broad band near 1450 cm^{-1} has been assigned to the CH_2 bending vibration of gauche conformers. In fact, it consists of two overlapping peaks at 1455 and 1440 cm^{-1} (both with $w \sim 16$ cm^{-1}) that Štokr suggested might correspond to Gt and Gg forms.[15] For the trans conformers this vibration shifts to 1471 cm^{-1}, but it is interesting to note that it is much broader for TX ($w = 28$ cm^{-1}) than for TC ($w = 8$ cm^{-1}). The CH_2 rocking band (Figure 14) shifts from 897 cm^{-1} in the G spectrum to around 848 cm^{-1} in the TX and TC spectra, in agreement with published transmission work. Again, it appears to be broader in TX ($w = 33$ cm^{-1}) than in TC ($w = 22$ cm^{-1}), but it is difficult to compare its position because of the high noise level in this region. The glycol C−O stretching band pair is also interesting (Figure 13). For the gauche conformers the maximum is observed at 1042 cm^{-1}; Štokr et al. assigned this band to the Gt form.[15] In fact, the peak fitting strongly suggests the presence of two rather broad peaks, one at 1045 cm^{-1} and one at 1026 cm^{-1}. The latter could possibly correspond to the Gg form, in analogy with the CH_2 bending vibration. In the trans spectra this vibration shifts to 972 cm^{-1}, but once again it is noticeably broader in the TX spectrum ($w = 21$ cm^{-1}) than in the TC spectrum ($w = 11$ cm^{-1}). The complexity of this band has already been recognized. Yazdanian et al.[27] decomposed it into three Lorentzian peaks: a main one at 973 cm^{-1} corresponding to load-bearing trans conformers in

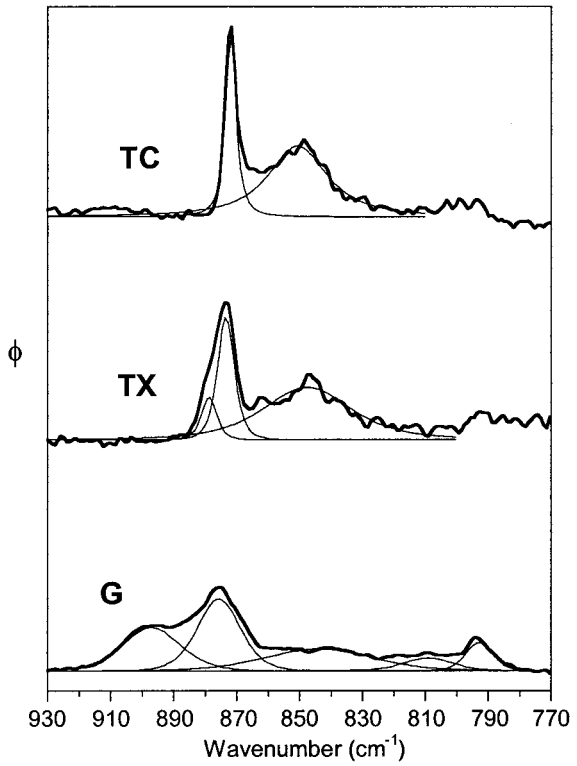

Figure 14. The 930−770 cm^{-1} region of the basis spectra of Figure 8.

"backbone" type crystals and two weaker peaks at 962 and 978 cm^{-1} corresponding to non-load-bearing trans conformers in "epitaxial" type crystals. Heuvel and Huisman,[94] on the other hand, decomposed it into two peaks with a Pearson VII shape, both near 972 cm^{-1} but one broad ($w \sim 30$ cm^{-1}) and one narrow ($w \sim 12$ cm^{-1}). The latter approach is more consistent with the

present analysis. The two components were assigned to amorphous and crystalline trans, respectively. Fina and Koenig[91] also observed that this band is much broader for a sample drawn at 80 °C than for a thermally crystallized sample, where it is accompanied by the chain folding band at 988 cm^{-1}. The 972 cm^{-1} band is particularly interesting because its position shifts significantly when stress is applied to the PET. Van den Heuvel et al.[95] showed that above 3% strain the "amorphous" component shifts much more than the "crystalline" component.

The remaining peaks in Figures 12−14 correspond to vibrations of the benzene ring. The band near 1020 cm^{-1} has been assigned to an in-plane bending mode of the ring C−H bonds.[14] Several groups have recognized that it involves at least two and probably three components.[13,21,89,96,97] The most detailed analysis is that of Yang et al.,[97] who decomposed it by means of peak fitting into three peaks at 1017.8 cm^{-1} (w = 7.0 cm^{-1}), 1021.5 cm^{-1} (w = 6.2 cm^{-1}), and 1024.2 cm^{-1} (w = 5.0 cm^{-1}) that they assigned respectively to gauche, amorphous trans, and crystalline trans conformers. These results match quite well the respective parameters for the separate G, TX, and TC spectra in Figure 13, which are as follows: 1017.7 cm^{-1} (w = 6.2 cm^{-1}), 1020.1 cm^{-1} (w = 6.3 cm^{-1}), and 1023.6 cm^{-1} (w = 5.2 cm^{-1}). The complexity of the out-of-plane C−H band at 875 cm^{-1} has also been recognized. Koenig and co-workers observed that it shifted and became narrower upon thermal crystallization.[13,21,28] Both Hutchinson et al.[89] and Heuvel and Huisman[94] analyzed it in terms of a narrow "ordered" component at 873 cm^{-1} and a broader "disordered" component at 878 cm^{-1}. The spectra in Figure 14 underline the complex behavior. In the G spectrum the peak occurs at 875.7 cm^{-1}, is close to symmetric, and is rather broad ($w \sim$ 16 cm^{-1}). In the TX spectrum the maximum shifts to 873.4 cm^{-1} and it becomes narrower, but there is an apparent shoulder around 879 cm^{-1} that requires an additional peak in the fitting. In the TC spectrum it shifts further still, to 871.9 cm^{-1}, and is symmetric and quite sharp (w = 3.8 cm^{-1}). The band at 1410 cm^{-1}, assigned to an in-plane vibration of the benzene ring,[12] has been mentioned previously in connection with its use as a reference band to normalize the spectra. Like the others, it is also sensitive to conformation. In the G spectrum it occurs at 1409.8 cm^{-1}, with a low-wavenumber tail that can be fit by a broader underlying peak at 1402 cm^{-1}. In the TX spectrum it shifts slightly lower, to 1408.7 cm^{-1}, but in the TC spectrum it reverts to a significantly higher value of 1412.2 cm^{-1}. However, the width remains constant throughout at about 8 cm^{-1}. Several earlier publications have provided evidence of at least two components for this band.[21,80,92,96] There are also indications that it possesses some degree of parallel dichroism.[8,98,99] Thus, it is not completely insensitive to conformation and orientation, but nevertheless it appears to be the best peak available for use as a reference band. The peak at 1505 cm^{-1}, also assigned to an in-plane ring vibration, behaves like the 1410 cm^{-1} band; it occurs at 1504.9 cm^{-1} (w = 7.2 cm^{-1}) in the G spectrum, 1504.3 cm^{-1} (w = 7.6 cm^{-1}) in the TX spectrum, and 1506.1 cm^{-1} (w = 3.9 cm^{-1}) in the TC spectrum. It is also sometimes used as a reference band because its intensity does not depend on the state of crystallinity,[99] but it is not insensitive to orientation,[88] as can be seen in Figure 3. The peak at 1386.0 cm^{-1} in the TC spectrum has been observed in crystalline PET and assigned to an in-plane C−H bending mode of the benzene ring.[6,8,9] It also appears to be present in the TX spectrum but occurs at 1380.2 cm^{-1} and is broader. Finally, there are the weak peaks at 1577, 1174, and 795 cm^{-1}; these have been assigned to benzene ring vibrations,[14] although Miyake suggested that the 1174 cm^{-1} peak might be due to CH_2 twisting.[6] The first two are associated with the amorphous phase of PET, their absence from the crystalline phase spectrum being attributed to its center of symmetry.[15] Although it is sensitive to orientation, the 795 cm^{-1} band has often been used as a reference[5,9,88,100] because it was believed to be independent of crystallinity. However, the results of Fina and Koenig indicated that it is associated with the gauche conformer and therefore the amorphous phase.[28] While it is difficult to be conclusive because of the noise level in Figure 8, our spectra do indicate that all three peaks are most intense in the G spectrum.

Our data in the wavenumber range 1600−1300 cm^{-1} are supported by transmission spectra in the literature.[101,102] For example, the spectra obtained by Qian et al. for PET thermally crystallized under different conditions (Figure 2 of ref 101) show the same trends seen in Figure 6; the growth of the trans CH_2 wagging peak near 1340 cm^{-1} is accompanied by the appearance of distinct peaks at 1471 and 1386 cm^{-1}. On the other hand, the spectra obtained by Sonoyama et al. (Figure 1 of ref 102) for PET films uniaxially drawn up to λ = 5 resemble Figure 4, in which the 1471 and 1386 cm^{-1} peaks are not clearly seen even though the trans wagging peak grows to the same extent as in the thermally crystallized samples. It is interesting to note that, in an earlier paper by Sonoyama et al.,[96] the spectrum of a film drawn to λ = 5 shows more prominent peaks at 1471 and 1386 cm^{-1}; this film may have been drawn at higher temperature or held at temperature a longer time before quenching. Similarly, Koenig and Hannon reported that the "crystalline" peak at 1386 cm^{-1} does not appear on drawing, whereas the 973 cm^{-1} peak does.[9] Our results show that both the 1471 and 1386 cm^{-1} peaks do appear on drawing but are not easily detected because they are broader, and the 1386 cm^{-1} peak is shifted to 1380 cm^{-1} and therefore hidden under the gauche wagging peak at 1370 cm^{-1}. These subtle differences have not been noticed before, to our knowledge, because the two types of samples (cold drawn and annealed) have not been analyzed as part of the same set and because the transmission spectra are often limited to those spectral regions where the peaks are not totally absorbing.

Figures 15 and 16 show the strong absorption bands in the range 1340−1060 cm^{-1}, mainly attributable to ester group vibrations. Like the carbonyl-related bands at 1727 and 730 cm^{-1}, these have received relatively little attention up to now because they are often saturated in transmission spectra. Although they are well-defined in the present set of spectra, interpretation is difficult because of the complexity and peak overlap. Nevertheless, it is possible to make some tentative peak fits and assignments. Boerio et al.[12] predicted five infrared-active bands in this range for the planar all trans PET structure: ring CC stretching at 1293 cm^{-1}, glycol O−C−H bending at 1271 cm^{-1}, complex in-plane ring-ester modes at 1254 and 1126 cm^{-1}, and a pure in-plane ring mode at 1102 cm^{-1}. Our TC spectrum clearly shows four peaks at 1278, 1259, 1132, and 1112

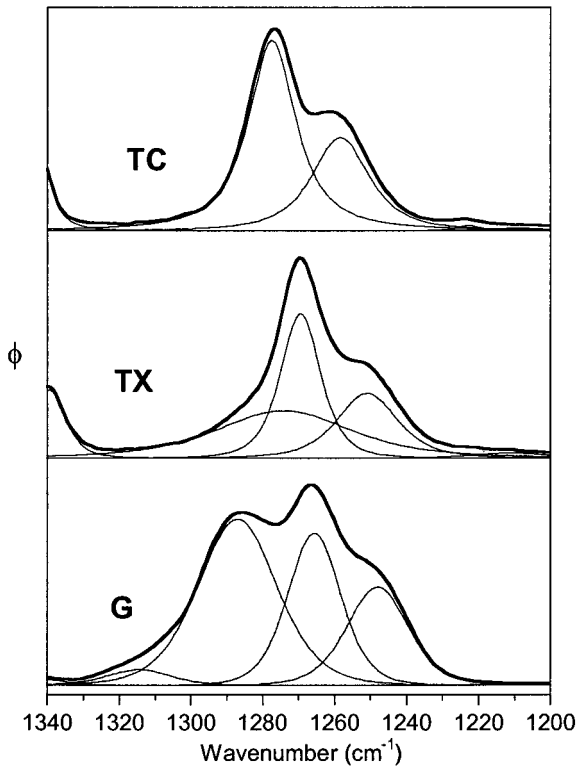

Figure 15. The 1340−1200 cm^{-1} region of the basis spectra of Figure 8.

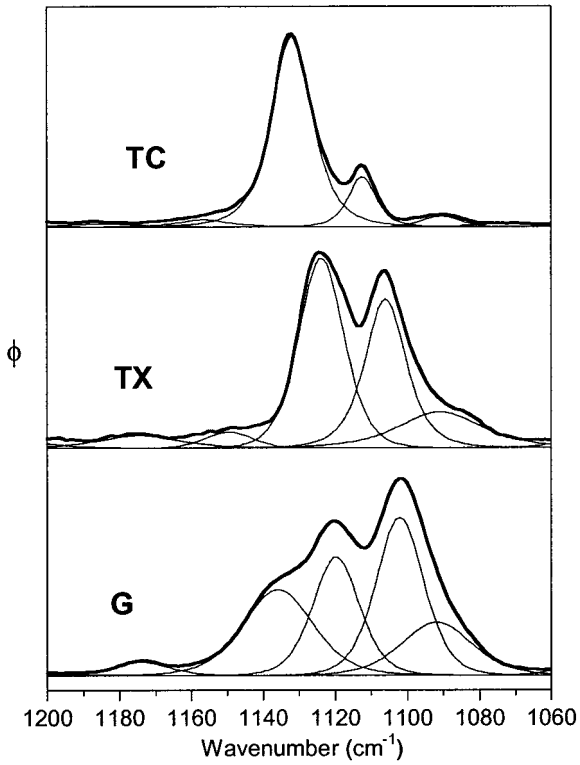

Figure 16. The 1180−1060 cm^{-1} region of the basis spectra of Figure 8.

cm^{-1} that we can assign to the latter four vibrations. The TX spectrum also shows four strong peaks that match those of the TC spectrum, except that they are all shifted to lower wavenumber (1270, 1251, 1124, and 1106 cm^{-1}). The G spectrum is more complicated. If we assume that the shift to lower wavenumber is related to increasing disorder and we extrapolate, then the four modes just mentioned can be assigned to the peaks at 1266, 1248, 1120, and 1102 cm^{-1}. This leaves the peaks at 1315, 1287, 1174, 1136, and 1092 cm^{-1} to be assigned. They no doubt correspond to modes that are both IR- and Raman-active for amorphous PET, with its predominance of gauche conformers, but only Raman-active for crystalline PET, with its centrosymmetric trans structure. The peak at 1092 cm^{-1} is probably due to the symmetric C−O stretch of the glycol group, assigned by Miyake[6] to the more obvious peak near 1099 cm^{-1}. The peak at 1174 cm^{-1} was assigned to a CH_2 twisting mode by Miyake[6] and to an in-plane ring mode by Ward and Wilding.[14] According to Boerio et al., both should occur near this frequency. The 1136 cm^{-1} peak may correspond to the other member of the pair, but it is difficult to make an exact assignment. The peaks at 1315 and 1287 cm^{-1} probably correspond respectively to the ring CCH and complex ring-ester modes observed in the Raman spectrum.[12]

Finally, it is interesting to note that in the dichroic difference spectrum of Figure 3 the positions and shapes of the dichroic peaks correspond to a mixture of the TX and TC spectra, with the TX spectrum predominating. This is consistent with the proportions of the TX and TC structures in the drawn samples (Table 2) and shows that both types of trans structures are significantly oriented while the gauche structures are not. The dichroism of the trans peaks is extensively used to quantify the orientation in PET, with the implicit assumption that all trans groups may be treated in the same manner. When both types are present, this is only an approximation, because for a given vibrational mode the two may not only have different intrinsic absorption intensities but may also involve different angles between the transition moment and the chain axis direction.

The preceding analysis provides some insight into the difference between drawn and thermally crystallized samples of PET but not into the difference between the two stages of thermal crystallization (below and above about 160 °C). It is clear from Figures 6 and 7 and Table 2 that even at the lower temperatures used to anneal the PET samples conformational rearrangement of carbonyls occurs along with gauche−trans conversion. This is confirmed by the work of Pastor et al.,[23,42,43] who showed that the Raman carbonyl bandwidth changes over both stages in a manner similar to that observed for the gauche and trans conformer content by Lin and Koenig.[21,37] The second stage of thermal crystallization is generally considered to correspond to an increase in the degree of crystal perfection.[36] According to some studies, this involves changes not only in chain folding, crystal size, lamella thickness, and the like but also in unit cell dimensions. For example, Kilian et al.[39] reported a significant decrease in certain lattice spacings in samples annealed above approximately 180 °C. Ramesh et al.[103] found that heat setting of PET fibers had a similar effect on the *a* and *b* dimensions of the unit cell, but more so on *a* (the dimension approximately normal to the benzene ring planes). Heuvel and Huisman[104] also found that the *a*-axis length decreased in fibers taken up at higher winding speeds and suggested that "the temperature at which the crystal forms influences the stacking of the molecules in the direction of the *a*-axis". To explore the two stages of thermal crystallization, another exercise was undertaken. As mentioned earlier, each of the experimental spectra can

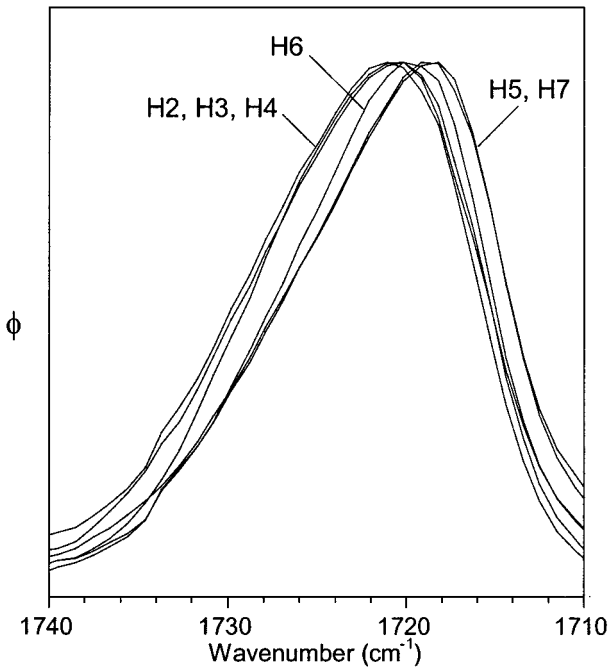

Figure 17. Carbonyl peak in the "residual" spectra for the heated samples (see text).

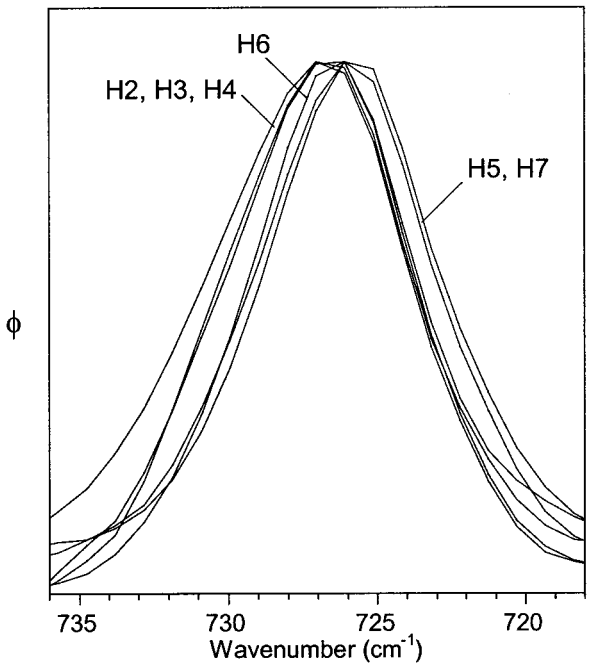

Figure 18. Out-of-plane bending peak in the "residual" spectra for the heated samples (see text).

be expressed as a sum of the three basis spectra G, TX, and TC in the proportions given in Table 2. If the contributions of the G and TX spectra are subtracted out, the residual spectrum should match TC. While this was true for most of the peaks, some subtle variations were observed for the carbonyl-related bands near 1720 and 730 cm^{-1}. Figure 17 compares the position of the carbonyl stretching band in the different residual spectra. For the samples annealed at 100 or 120 °C (H2, H3, H4) the maximum is close to 1720.8 cm^{-1}. For the ones annealed at 200 °C (H5) or slowly cooled from the melt (H7) it occurs at 1718.7 cm^{-1}. For the one annealed at 160 °C (H6) it is intermediate and occurs at 1719.8 cm^{-1}, the same value as in the TC spectrum. Similar behavior is observed for the low-wavenumber bending peak (Figure 18), although the shifts are smaller. These variations are believed to be significant, although too subtle to show up clearly as a fourth factor in the factor analysis. As proposed by Heuvel and Huisman,[104] higher temperature crystallization leads to more efficient packing of the molecular chains, and this affects the vibrational frequencies of the carbonyl group. Thus, within the TC "crystalline" structure there is a variation in the nature of the order at the molecular level that is related to the temperature of crystallization. It should be noted that this variation does not always parallel the degree of crystallinity, as expressed in terms of the trans conformer content. For example, sample H6 (annealed at 160 °C for 24 h) contains more of both the disordered TX and the crystalline TC structures than sample H5 (annealed at 200 °C for 15 min), but the TC structure in H6 is less highly ordered than it is in H5.

General Discussion and Conclusions. On the basis of the preceding results, we can add some details to the model proposed by D'Esposito and Koenig to describe the development of crystalline order in PET.[13]

Amorphous PET consists of random chains in which the glycol groups exist primarily (about 85%) in the gauche (G) form, so the trans (T) conformers are for the most part isolated units. The gauche and trans conformers give rise to different vibrational spectra. The carbonyl bonds of the terephthalate moiety are in a disordered arrangement with respect to the benzene rings, but it is still not clear whether this involves nonplanar conformations or a mixture of cis (C_B) and trans (T_B) planar conformations. On the basis of the broad Gaussian shape of the carbonyl band in the Raman spectrum (also observed here in the IR spectrum), Melveger suggested a distribution of nonplanar arrangements.[33] Štokr et al., on the other hand, suggested an approximately equal mixture of cis and trans.[15]

The transformation of amorphous PET to crystalline PET essentially involves three distinct processes at the molecular level that do not necessarily occur simultaneously and may be arranged in order of ease of achievement as follows: (1) conversion of gauche (G) glycol conformers to trans (T); (2) ordering of the terephthalate moiety through rearrangement of the carbonyl groups with respect to the benzene rings and possibly also rotation around the C−O bonds from gauche (g) to trans (t); (3) a third rearrangement that accounts for the more efficient packing observed at high temperatures.

When amorphous PET is drawn in the solid state, the few trans glycol units initially present quickly become oriented. This is followed by conversion of gauche units to new oriented trans units. Under certain conditions (like relatively low draw temperature and draw rate) there is little change in the conformation of the terephthalate moiety, and the overall effect is simply an increase in the number of trans units. When there are enough of them to form extended oriented linear sequences, they tend to align to form an ordered structure. This is the problematic intermediate phase that is so hard to describe. Because the terephthalate moieties do not possess the required all-T_B regularity, it differs from the true crystalline phase and is sometimes described as amorphous, particularly when it is characterized by X-ray diffraction. This is not correct, however, because it is considerably more ordered than the true amorphous phase and when characterized by DSC will appear quite

Table 4. Structural Entities Present in PET

entity	phase	glycol conformation	terephthalate conformation	spectrum
1	amorphous	gauche	disordered	G
2	amorphous	trans (isolated)	disordered	TX (and G?)
3	intermediate	trans (extended)	disordered	TX
4	crystalline	trans (extended)	ordered	TC
5	crystalline (chain folds)	gauche	disordered	G (and TC?)

crystalline. Its density is expected to be higher than that of the amorphous phase but lower than that of the crystalline phase. This is confirmed by the results in Figure 12 of ref 100, where the increase in density as a function of trans content follows two distinct curves for drawn films and heat-set nondrawn films.

If the drawing is done at higher temperature or draw rate, or the PET is thermally crystallized, then rearrangement of the terephthalate moiety is facilitated. This allows the chains to pack more efficiently into the true crystalline structure. However, the intermediate phase is still present, although not to the same extent as in cold-drawn samples. On the other hand, the intermediate phase could be very significant in fibers spun from the molten state, where the orientation produced on passing through the die will bring about G-to-T conversion, but if there is rapid quenching, there may be little time for significant terephthalate rearrangement. This however would be expected to occur on subsequent heat setting.

Several ^{13}C NMR studies have also provided evidence for formation of such an intermediate phase.[71,72,75,105] Both the ethylene glycol and carbonyl peaks show two partially overlapping resonances: a relatively broad low-field component corresponding to a disordered state and a narrower high-field component corresponding to a more ordered state. As for the IR spectra discussed here, cold drawing was found to produce significant changes in the ethylene glycol peak but none in the carbonyl or aromatic ring peaks, although the latter do change on annealing.[71,72,75] In fact, the changes in the carbonyl peak shape are surprisingly similar to those seen in the IR spectra.[75] Even for a set of samples obtained by thermal annealing only (no drawing), Huang et al.[76] concluded that gauche-to-trans conversion proceeds before subsequent crystallization and proposed a model involving three domains: amorphous (gauche rich), constrained noncrystalline (trans rich), and crystalline (all trans).

A sample of PET may therefore be considered to contain varying amounts of five different structural entities, summarized in Table 4. In addition to the four entities already discussed, the table includes the chain folds associated with the crystalline lamellae. These were studied by Fina and Koenig,[106] who concluded that each fold contains between two and three G conformers and negligible T conformers. It is reasonable to expect some "disorder" (i.e., non-T_B conformations) for the terephthalate groups in the chain folds as well. Each of the five entities would be expected to possess a distinct IR spectrum, but in some cases the differences may be small. This would explain why we have been able to isolate only three spectra, which may not be entirely "pure". Our spectrum TX corresponds to both the isolated trans units found in the amorphous phase and the extended trans units found in the intermediate phase (hence the difficulty in finding a label to describe it), but a subtle difference between the two may explain why our G spectrum contains some weak trans features. These could represent a small difference between the truly amorphous trans and the intermediate trans. Likewise, our G spectrum should include the gauche units found in both the amorphous phase and the chain folds, but again subtle differences may explain some aspects of our TC spectrum. As mentioned previously, crystalline PET is believed to involve only the T_B arrangement for the terephthalate groups.[16] In both the C_B and T_B arrangements, the two carbonyls adjacent to a benzene ring will give rise to two vibrational modes, in-phase and out-of-phase. However, because of the center of symmetry present in the T_B arrangement, only the out-of-phase mode will be infrared-active. Hence, a well-organized T_B structure should show only a single carbonyl peak in the infrared spectrum, but our TC spectrum shows a distinctly asymmetric carbonyl band (Figure 9). The high-wavenumber shoulder may be due to a difference between the C_B arrangements associated with chain folds and those associated with the other structures. As shown by Fina and Koenig,[106] the increase in order observed in samples annealed above 160 °C is due at least in part to an increase in lamellar thickness, with a concomitant decrease in the relative number of chain folds. An associated decrease in C_B conformations could explain the change in carbonyl peak shape shown in Figure 17.

The presence of an intermediate structure involving extended trans sequences with disordered terephthalate groups can help to explain several anomalies associated with PET, in addition to the apparent discrepancy among the crystallinity values determined by different methods. Such anomalies are often more pronounced when the samples studied include fibers or drawn material, where the intermediate phase can be more abundant. A case in point is the use of the pair of peaks at 1473 and 1455 cm^{-1} (CH_2 deformation, trans and gauche) to determine crystallinity in PET. Belali and Vigoureux[107] used this approach for a set of three films (amorphous, uniaxially drawn, biaxially drawn) and found a poor correlation. Examination of their Figure 4 in the light of the present work shows why. Both drawn films show a fairly high trans content, as indicated by the CH_2 wagging peak near 1340 cm^{-1}. The biaxially drawn film also shows a peak at 1386 cm^{-1} and a sharp peak at 1473 cm^{-1}, as in our TC spectrum, showing that the trans groups exist mainly in the fully formed crystalline structure. The uniaxially drawn film, on the other hand, does not show these peaks, because the trans groups are mostly in the intermediate-type structure, where the peak at 1473 cm^{-1} is much broader and less obvious, as in our TX spectrum. As a result, using the height of the 1473 cm^{-1} peak does not give reliable results. This was not the case for Gruver et al.,[108] who found that the 1470/1450 cm^{-1} peak ratio correlated well with XRD and density results. However, their study involved only heat-treated samples, in which the intermediate trans content presumably remained low enough so as not to cause a poor correlation. Similar anomalies have been observed in Raman spectroscopy and can be explained in the same way. Both the width of the carbonyl band and the intensity of a peak at 1096 cm^{-1}

have been used as a measure of the degree of crystallinity.[33,109,110] The results of Ellis et al.[63] indicate that while thermal annealing produces a strong peak at 1096 cm^{-1} (presumably associated with crystalline trans), drawing produces only a weak peak accompanied by others at 1084 and 1066 cm^{-1} (associated with intermediate trans). Since both the 1096 cm^{-1} peak and the carbonyl bandwidth are associated with the true crystalline structure, they show a good correlation with each other,[109] but when either one is plotted against density, different relationships are observed for drawn and isotropic (heat crystallized) samples.[33,110] The same variations in the 1150−1050 cm^{-1} region of the Raman spectrum are seen for PET spun fibers, where low take-up speeds seem to favor the intermediate trans structure while higher speeds favor the crystalline trans structure.[111,112]

These are only a few examples of PET behavior that may be explained in terms of the conformational changes suggested by our analysis of the IR spectrum. Although the gauche−trans conversion of the glycol groups is undisputedly important, the "changes in the symmetry and resonance characteristics of the substituted benzenoid framework" proposed by Liang and Krimm[7] are by no means insignificant. The information obtained in this work should thus prove valuable with respect to the use of IR spectroscopy as a tool to study the structure of PET.

Acknowledgment. The authors are grateful to Ms. Ana Delgado and Dr. Ralph Paroli of NRC's Institute for Research in Construction, Ottawa, for making possible the Raman measurements.

References and Notes

(1) Ward, I. M. *Chem. Ind.* **1956**, 905−906.
(2) Ward, I. M. *Chem. Ind.* **1957**, 1102.
(3) Grime, D.; Ward, I. M. *Trans. Faraday Soc.* **1958**, *54*, 959−971.
(4) Daniels, W. W.; Kitson, R. E. *J. Polym. Sci.* **1958**, *33*, 161−170.
(5) Miyake, A. *J. Polym. Sci.* **1959**, *38*, 479−495.
(6) Miyake, A. *J. Polym. Sci.* **1959**, *38*, 497−512.
(7) Liang, C. Y.; Krimm, S. *J. Mol. Spectrosc.* **1959**, *3*, 554−574.
(8) Krimm, S. *Adv. Polym. Sci.* **1960**, *2*, 51−172.
(9) Koenig, J. L.; Hannon, M. J. *J. Macromol. Sci., Part B* **1967**, *B1*, 119−145.
(10) Manley, T. R.; Williams, D. A. *Polymer* **1969**, *10*, 339−384.
(11) Bahl, S. K.; Cornell, D. D.; Boerio, F. J.; McGraw, G. E. *J. Polym. Sci., Polym. Lett. Ed.* **1974**, *12*, 13−19.
(12) Boerio, F. J.; Bahl, S. K.; McGraw, G. E. *J. Polym. Sci., Polym. Phys. Ed.* **1976**, *14*, 1029−1046.
(13) D'Esposito, L.; Koenig, J. L. *J. Polym. Sci., Polym. Phys. Ed.* **1976**, *14*, 1731−1741.
(14) Ward, I. M.; Wilding, M. A. *Polymer* **1977**, *18*, 327−335.
(15) Štokr, J.; Schneider, B.; Doskocilová, D.; Lövy, J.; Sedlácek, P. *Polymer* **1982**, *23*, 714−721.
(16) Daubeny, R. de P.; Bunn, C. W.; Brown, C. J. *Proc. R. Soc. London* **1954**, *226A*, 531−542.
(17) Auriemma, F.; Corradini, P.; De Rosa, C.; Guerra, G.; Petraccone, V.; Bianchi, R.; Di Dino, G. *Macromolecules* **1992**, *25*, 2490−2497.
(18) Alemán, C.; Muñoz-Guerra, S. *J. Polym. Sci., Part B: Polym. Phys.* **1996**, *34*, 963−973.
(19) Nicholson, T. M.; Davies, G. R.; Ward, I. M. *Polymer* **1994**, *35*, 4259−4262.
(20) Carr, P. L.; Nicholson, T. M.; Ward, I. M. *Polym. Adv. Technol.* **1997**, *8*, 592−600.
(21) Lin, S.-B.; Koenig, J. L. *J. Polym. Sci., Polym. Phys. Ed.* **1982**, *20*, 2277−2295.
(22) Aharoni, S. M.; Sharma, R. K.; Szobota, J. S.; Vernick, D. A. *J. Appl. Polym. Sci.* **1983**, *28*, 2177−2186.
(23) Rodríguez-Cabello, J. C.; Quintanilla, L.; Pastor, J. M. *J. Raman Spectrosc.* **1994**, *25*, 335−344.
(24) Wang, Y.; Shen, D.; Qian, R. *J. Polym. Sci., Part B: Polym. Phys.* **1998**, *36*, 783−788.
(25) Heffelfinger, C. J.; Schmidt, P. G. *J. Appl. Polym. Sci.* **1965**, *9*, 2661−2680.
(26) Cunningham, A.; Ward, I. M.; Willis, H. A.; Zichy, V. *Polymer* **1974**, *15*, 749−756.
(27) Yazdanian, M.; Ward, I. M.; Brody, H. *Polymer* **1985**, *26*, 1779−1790.
(28) Fina, L. J.; Koenig, J. L. *J. Polym. Sci., Part B: Polym. Phys.* **1986**, *24*, 2525−2539.
(29) Spiby, P.; O'Neill, M. A.; Duckett, R. A.; Ward, I. M. *Polymer* **1992**, *33*, 4479−4485.
(30) Ajji, A.; Guèvremont, J.; Cole, K. C.; Dumoulin, M. M. *Polymer* **1996**, *37*, 3707−3714.
(31) Schmidt-Rohr, K.; Hu, W.; Zumbulyadis, N. *Science* **1998**, *280*, 714−717.
(32) Williams, A. D.; Flory, P. J. *J. Polym. Sci., Part A-2* **1967**, *5*, 417−424.
(33) Melveger, A. *J. Polym. Sci., Part A-2* **1972**, *10*, 317−322.
(34) Tonelli, A. E. *J. Polym. Sci., Polym. Lett. Ed.* **1973**, *11*, 441−447.
(35) Purvis, J.; Bower, D. I. *J. Polym. Sci., Polym. Phys. Ed.* **1976**, *14*, 1461−1484.
(36) Jog, J. P. *J. Macromol. Sci., Rev. Macromol. Chem. Phys.* **1995**, *C35*, 531−553.
(37) Lin, S.-B.; Koenig, J. L. *J. Polym. Sci., Polym. Phys. Ed.* **1983**, *21*, 2365−2378.
(38) Lin, S.-B.; Koenig, J. L. *J. Polym. Sci., Polym. Symp.* **1984**, *71*, 121−135.
(39) Kilian, H. G.; Halboth, H.; Jenckel, E. *Kolloid-Z.* **1960**, *172*, 166−177.
(40) Zachmann, H. G.; Schmidt, G. F. *Makromol. Chem.* **1962**, *52*, 23−36.
(41) Bonart, R. *Kolloid Z. Z. Polym.* **1966**, *213*, 1−11.
(42) Pastor, J. M.; González, A.; De Saja, J. A. *J. Appl. Polym. Sci.* **1989**, *38*, 2283−2288.
(43) Quintanilla, L.; Rodríguez-Cabello, J. C.; Jawhari, T.; Pastor, J. M. *Polymer* **1993**, *34*, 3787−3795.
(44) Terada, T.; Sawatari, C.; Chigono, T.; Matsuo, M. *Macromolecules* **1982**, *15*, 998−1004.
(45) LeBourvellec, G.; Monnerie, L.; Jarry, J. P. *Polymer* **1986**, *27*, 856−860.
(46) Dargent, E.; Grenet, J.; Auvray, X. *J. Therm. Anal.* **1994**, *41*, 1409−1415.
(47) Salem, D. *Polymer* **1998**, *39*, 7067−7077.
(48) Misra, A.; Stein, R. S. *J. Polym. Sci., Polym. Phys. Ed.* **1979**, *17*, 235−257.
(49) Gupta, V. B.; Jain, A. K.; Radhakrishnan, J.; Chidambareswaran, P. K. *J. Macromol. Sci., Part B* **1994**, *B33*, 185−207.
(50) Rodríguez-Cabello, J. C.; Merino, J. C.; Fernández, M. R.; Pastor, J. M. *J. Raman Spectrosc.* **1996**, *27*, 23−29.
(51) Rodríguez-Cabello, J. C.; Merino, J. C.; Quintanilla, L.; Pastor, J. M. *J. Appl. Polym. Sci.* **1996**, *62*, 1953−1964.
(52) Vigny, M.; Tassin, J. F.; Gibaud, A.; Lorentz, G. *Polym. Eng. Sci.* **1997**, *37*, 1785−1794.
(53) Dargent, E.; Grenet, J.; Dahoun, A. *Polym. Eng. Sci.* **1997**, *37*, 1853−1857.
(54) Vigny, M.; Tassin, J. F.; Lorentz, G. *Polymer* **1999**, *40*, 397−406.
(55) Radhakrishnan, J.; Gupta, V. B. *J. Macromol. Sci., Part B* **1993**, *B32*, 243−259.
(56) Lindner, W. L. *Polymer* **1973**, *14*, 9−15.
(57) Gupta, V. B.; Kumar, S. *Polymer* **1978**, *19*, 953−955.
(58) Wu, G.; Jiang, J.-D.; Tucker, P. A.; Cuculo, J. A. *J. Polym. Sci., Part B: Polym. Phys.* **1996**, *34*, 2035−2047.
(59) Fu, Y.; Busing, W. R.; Jin, Y.; Affholter, K. A.; Wunderlich, B. *Macromol. Chem. Phys.* **1994**, *195*, 803−822.
(60) Farrow, G.; Ward, I. M. *Polymer* **1960**, *1*, 330−339.
(61) Sharma, V.; Desai, P.; Abhiraman, A. S. *J. Appl. Polym. Sci.* **1997**, *65*, 2603−2612.
(62) Murthy, N. S.; Correale, S. T.; Minor, H. *Macromolecules* **1991**, *24*, 1185−1189.
(63) Ellis, G.; Román, F.; Marco, C.; Gómez, M. A.; Fatou, J. G. *Spectrochim. Acta, Part A* **1995**, *51*, 2139−2145.
(64) Bai, C.; Spontak, R. J.; Koch, C. C.; Saw, C. K.; Balik, C. M. *Polymer* **2000**, *41*, 7147−7157.
(65) Asano, T.; Baltá Calleja, F. J.; Flores, A.; Tanigaki, M.; Forhad Mina, M.; Sawatari, C.; Itagaki, H.; Takahashi, H.; Hatta, I. *Polymer* **1999**, *40*, 6475−6484.
(66) Radhakrishnan, J.; Kaito, A. *Polymer* **2001**, *42*, 3859−3866.
(67) Imai, M.; Mori, K.; Mizukami, T.; Kaji, K.; Kanaya, T. *Polymer* **1992**, *33*, 4451−4456.

(68) Imai, M.; Mori, K.; Mizukami, T.; Kaji, K.; Kanaya, T. *Polymer* **1992**, *33*, 4457−4462.
(69) Imai, M.; Kaji, K.; Kanaya, T. *Macromolecules* **1994**, *27*, 7103−7108.
(70) Havens, J. R.; VanderHart, D. L. *Macromolecules* **1985**, *18*, 1663−1676.
(71) Tzou, D. L.; Desai, P.; Abhiraman, A. S.; Huang, T.-H. *J. Polym. Sci., Part B: Polym. Phys.* **1991**, *29*, 49−56.
(72) Tzou, D. L.; Desai, P.; Abhiraman, A. S.; Huang, T.-H. *J. Polym. Sci., Part B: Polym. Phys.* **1995**, *33*, 63−69.
(73) Wilhelm, M.; Spiess, H. W. *Macromolecules* **1996**, *29*, 1088−1090.
(74) Kawaguchi, T.; Mamada, A.; Hosokawa, Y.; Horii, F. *Polymer* **1998**, *39*, 2725−2732.
(75) Miwa, Y.; Takahashi, Y.; Kitano, Y.; Ishida, H. *J. Mol. Struct.* **1998**, *441*, 295−301.
(76) Huang, J.-M.; Chu, P. P.; Chang, F.-C. *Polymer* **2000**, *41*, 1741−1748.
(77) Mahendrasingam, A.; Martin, C.; Fuller, W.; Blundell, D. J.; Oldman, R. J.; MacKerron, D. H.; Harvie, J. L.; Riekel, C. *Polymer* **2000**, *41*, 1217−1221.
(78) Blundell, D. J.; Mahendrasingam, A.; Martin, C.; Fuller, W.; MacKerron, D. H.; Harvie, J. L.; Oldman, R. J.; Riekel, C. *Polymer* **2000**, *41*, 7793−7802.
(79) Mahendrasingam, A.; Blundell, D. J.; Martin, C.; Fuller, W.; MacKerron, D. H.; Harvie, J. L.; Oldman, R. J.; Riekel, C. *Polymer* **2000**, *41*, 7803−7814.
(80) Cole, K. C.; Guèvremont, J.; Ajji, A.; Dumoulin, M. M. *Appl. Spectrosc.* **1994**, *48*, 1513−1521.
(81) Guèvremont, J.; Ajji, A.; Cole, K. C.; Dumoulin, M. M. *Polymer* **1995**, *36*, 3385−3392.
(82) Kaito, A.; Nakayama, K. *Macromolecules* **1992**, *25*, 4882−4887.
(83) Bensaad, S.; Jasse, B.; Noël, C. *Polymer* **1993**, *34*, 1602−1605.
(84) Jansen, J. A. J.; Paridaans, F. N.; Heynderickx, I. E. J. *Polymer* **1994**, *35*, 2970−2976.
(85) Everall, N. J.; Chalmers, J. M.; Local, A.; Allen, S. *Vib. Spectrosc.* **1996**, *10*, 253−259.
(86) Cole, K. C.; Ajji, A.; Pellerin, E. *AIP (Am. Inst. Phys.) Conf. Proc.* **1998**, *430*, 571−574.
(87) Bertie, J. E.; Zhang, S. L.; Keefe, C. D. *J. Mol. Struct.* **1994**, *324*, 157−176.
(88) Walls, D. J. *Appl. Spectrosc.* **1991**, *45*, 1193−1198.
(89) Hutchinson, I. J.; Ward, I. M.; Willis, H. A.; Zichy, V. *Polymer* **1980**, *21*, 55−65.
(90) Garton, A.; Carlsson, D. J.; Holmes, L. L.; Wiles, D. M. *J. Appl. Polym. Sci.* **1980**, *25*, 1505−1507.
(91) Fina, L. J.; Koenig, J. L. *J. Polym. Sci., Part B: Polym. Phys.* **1986**, *24*, 2509−2524.
(92) Liu, J.; Koenig, J. L. *Anal. Chem.* **1987**, *59*, 2609−2615.
(93) Shen, D.; Yang, X.; Zhu, S.; Wu, Q.; Wen, Z. *Gaofenzi Tongxun* **1980** (*4*), 209−213.
(94) Heuvel, H. M.; Huisman, R. *J. Appl. Polym. Sci.* **1985**, *30*, 3069−3093.
(95) Van den Heuvel, C. J. M.; Heuvel, H. M.; Faassen, W. A.; Veurink, J.; Lucas, L. J. *J. Appl. Polym. Sci.* **1993**, *49*, 925−934.
(96) Sonoyama, M.; Shoda, K.; Katagiri, G.; Ishida, H. *Appl. Spectrosc.* **1996**, *50*, 377−381.
(97) Yang, X.; Long, F.; Shen, D.; Qian, R. *Polym. Commun.* **1991**, *32*, 125−128.
(98) Jain, A. K.; Gupta, V. B. *J. Appl. Polym. Sci.* **1990**, *41*, 2931−2939.
(99) Hoffmann, U.; Pfeifer, F.; Merino, J. C.; Okretic, S.; Pastor, J. M.; Rodríguez-Cabello, J. C.; Völkl, N.; Zahedi, M.; Siesler, H. W. *Appl. Spectrosc.* **1993**, *47*, 1531−1539.
(100) Schmidt, P. G. *J. Polym. Sci., Part A* **1963**, *1*, 1271−1292.
(101) Qian, R.; Shen, D.; Sun, F.; Wu, L. *Macromol. Chem. Phys.* **1996**, *197*, 1485−1493.
(102) Sonoyama, M.; Shoda, K.; Katagiri, G.; Ishida, H. *Appl. Spectrosc.* **1997**, *51*, 346−349.
(103) Ramesh, C.; Gupta, V. B.; Radhakrishnan, J. *J. Macromol. Sci., Part B* **1997**, *B36*, 281−299.
(104) Heuvel, H. M.; Huisman, R. *J. Appl. Polym. Sci.* **1978**, *22*, 2229−2243.
(105) Yamato, M.; Ezure, H.; Ito, E. *Kobunshi Ronbunshu* **1993**, *50*, 659−664.
(106) Fina, L. J.; Koenig, J. L. *Macromolecules* **1984**, *17*, 2572−2579.
(107) Belali, R.; Vigoureux, J. M. *Appl. Spectrosc.* **1994**, *48*, 465−471.
(108) Gruver, V.; Showers, D.; Kao, M.-Y.; Klebanov, L. *Proc. ANTEC (Society of Plastics Engineers Annual Technical Conference)* **2000**, 1636−1640.
(109) Bulkin, B. J.; Lewin, M.; DeBlase, F. J. *Macromolecules* **1985**, *18*, 2587−2594.
(110) Everall, N.; Tayler, P.; Chalmers, J. M.; MacKerron, D.; Ferwerda, R.; van der Maas, J. H. *Polymer* **1994**, *35*, 3184−3192.
(111) Adar, F.; Noether, H. *Polymer* **1985**, *26*, 1935−1943.
(112) Lesko, C. C. C.; Rabolt, J. F.; Ikeda, R. M.; Chase, B.; Kennedy, A. *J. Mol. Struct.* **2000**, *521*, 127−136.

MA011492I